Computers, Materials & Continua CMC, vol.62, no.3, pp.1001-1023, 2020

Free Vibration Analysis of FG-CNTRC Cylindrical Pressure Vessels Resting on Pasternak Foundation with Various Boundary Conditions

Mohammad Arefi[1], Masoud Mohammadi[1], Ali Tabatabaeian[1] and Timon Rabczuk[2, *]

Abstract: This study focuses on vibration analysis of cylindrical pressure vessels constructed by functionally graded carbon nanotube reinforced composites (FG-CNTRC). The vessel is under internal pressure and surrounded by a Pasternak foundation. This investigation was founded based on two-dimensional elastic analysis and used Hamilton's principle to drive the governing equations. The deformations and effective-mechanical properties of the reinforced structure were elicited from the first-order shear theory (FSDT) and rule of mixture, respectively. The main goal of this study is to show the effects of various design parameters such as boundary conditions, reinforcement distribution, foundation parameters, and aspect ratio on the free vibration characteristics of the structure.

Keywords: FG-CNTRC cylindrical pressure vessel, first-ordershear deformation theory, free vibration, Pasternak's foundation, rule of mixture.

1 Introduction

Pressure vessels construct an essential part of industrial equipment. They are under high levels of stresses and temperatures. Also, one of the expensive tools in an industrial unit is the pressure vessel. These critical points caused researchers and companies to release analyzing approaches and design guidelines for pressure vessels. More recently, one of the popular subjects is to use of composite materials, especially functionally graded materials (FGMs), for fabricating pressure vessels and other industrial equipment [Miao, Chen, Wang et al. (2014)].

Functionally graded carbon nanotube reinforced composites (FG-CNTRCs) were comprehensively analyzed for various functions. They showed a strong bending performance and reducing effects on residual stresses [Arefi, Faegh and Loghman (2016)]. All of these studies expressed that addition of carbon nanotubes into the base material increases stiffness of the structure and decreases deflections.

[1] Department of Solid Mechanic, Faculty of Mechanical Engineering, University of Kashan, Kashan 87317-51167, Iran.

[2] Duy Tan University, Institute of Research & Development, 3 Quang Trung, Danang, Vietnam.

[*] Corresponding Author: Timon Rabczuk. Email: timon.rabczuk@uni-weimar.de.

Keeping a far distance between working frequency and the natural frequency of industrial equipment is acrucial issue, which was widely considered by engineers. Accordingly, researchers widely focused on analyzing free vibration and forced vibration of industrial tools.

Many other researchers also considered vibration response of the composite materials in various structures, and developed their investigations around vibration analysis of cylindrical composites [SafarPour, Ghanbari and Ghadiri (2019); Zhao, Choe, Shuai et al. (2019)], composite plates and beams [Tan, Nguyen-Thanh, Rabczuk et al. (2018); Abualnour, Houari, Akgöz et al. (2017); Feng, Kitipornchai and Yang (2017); Kiani (2016); Sayyad and Ghugal (2017)], FG-CNTRC panels [Mirzaei and Kiani (2016)], and experimentally vibrational analysis on composite shells [Kalnins and Wieder (2017)].

A comprehensive literature review has been completed above. The literature review indicates that although some important works about FG-CNTRC structures have been published, there isa lack of work about two-dimensional free vibration responses of FG-CNTRC cylindrical pressure vessels with various boundary conditions. In this paper, first-order shear deformation theory is used to derive governing equations of motion. The equations are solved using a method for various boundary conditions. The main outcome of this paper is to clarify the influence of various distributions of reinforcement and various boundary conditions on the vibration behavior of the system.

2 Problem definition

2.1 CNT distribution

Fig. (1) shows the geometry of CNTRC cylindrical shell. The CNT volume fraction changes along the thickness to form a functionally graded structure. This study uses four different distribution patterns which are presented in Eq. (1) and shown in Fig. (2).

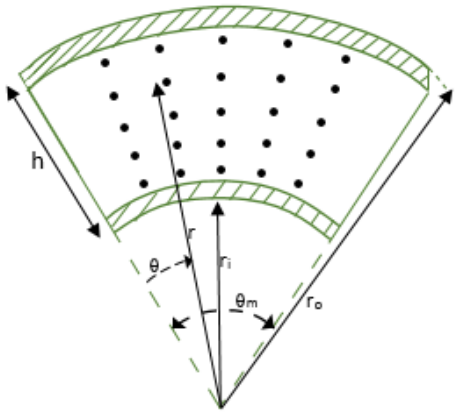

Figure 1: Geometry of CNTRC cylindrical shell

$$\begin{cases} pattern\ 1 & V_{CNT} = V_{CNT}^{*} & UD \\ pattern\ 2 & V_{CNT} = 2\left(\dfrac{r-R}{h} + 0.5\right)V_{CNT}^{*} & FG-\nabla \\ pattern\ 3 & V_{CNT} = 2\left(-\dfrac{r-R}{h} + 0.5\right)V_{CNT}^{*} & FG-\Delta \\ pattern\ 4 & V_{CNT} = 4\left(\dfrac{|r-R|}{h}\right)V_{CNT}^{*} & FG-X \end{cases} \tag{1}$$

where R, r, h are the average radius, variable radius, and thickness, respectively. Also V_{CNT} is a function of distribution of CNT for each specific pattern and V_{CNT}^{*} is the total volume fraction across the shell thickness that can be obtained as follows.

$$V_{CNT}^{*} = \frac{W_{CN}}{W_{CN} + \left(\frac{\rho_{CN}}{\rho_m}\right) - \left(\frac{\rho_{CN}}{\rho_m}\right)W_{CN}} \tag{2}$$

It should be noticed that W_{CN}, ρ_{CN}, ρ_m are respectively the weight fraction of the CNTs, density of the CNTs, and density of the matrix.

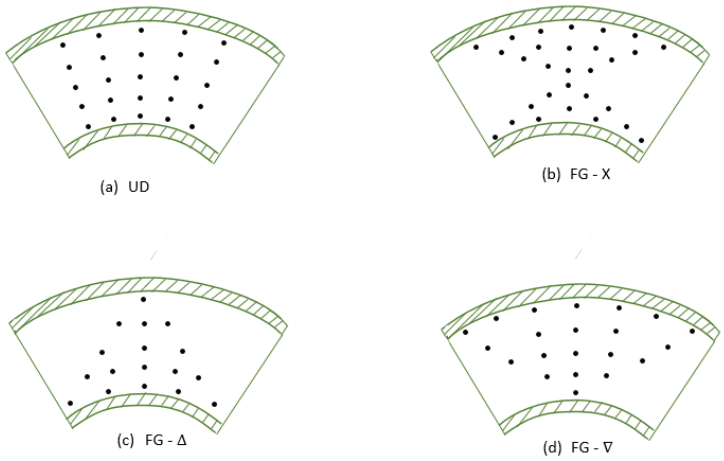

Figure 2: Different CNT distribution patterns

2.2 Effective material properties

The effective Young's modulus of the FG-cylindrical shell could be obtained using rule of mixture as [Asadi, Souri and Wang (2017)]:

$$E_{11} = \eta_1 V_{CNT} E_{11}^{CNT} + V_m E^m \tag{3}$$

$$\frac{\eta_2}{E_{22}} = \frac{V_{CNT}}{E_{22}^{CNT}} + \frac{V_m}{E^m} \tag{4}$$

$$\frac{\eta_3}{G_{12}} = \frac{V_{CNT}}{G_{12}^{CNT}} + \frac{V_m}{G^m} \tag{5}$$

$$V_{CNT} + V_m = 1 \tag{6}$$

$$\rho = V_{CNT}\rho^{CNT} + V_m\rho^m \tag{7}$$

$$\nu_{12} = V_{CNT}^{*}\nu_{12}^{CNT} + V_m\nu^m \tag{8}$$

in which η_1, η_2, and η_3 are certain quantities that called efficiency parameters.$E, G,$ and $\nu$are Young's modulus, shear modulus and Poisson's ratio, respectively. V and ρ represent volume fraction and density. Other effective mechanical properties are presented as follows:

$$\begin{aligned} E_{33} &= E_{22} \\ G_{13} &= G_{12} \\ \nu_{31} &= \nu_{21} \\ \nu_{32} &= \nu_{21} \end{aligned} \tag{9}$$

3 Theoretical formulations

3.1 Displacement field

First-order shear deformation theory (FSDT)is proposed for describing deformations and deflections as follows.

$$\begin{Bmatrix} u_x \\ w_z \end{Bmatrix} = \begin{Bmatrix} u(x,t) \\ w(x,t) \end{Bmatrix} + z\begin{Bmatrix} \varphi_x(x,t) \\ \varphi_z(x,t) \end{Bmatrix} \tag{10}$$

where u_x, w_z are the axial and radial components of displacement, respectively. u, w, φ_x, and φ_z are axial component, radial componentand rotational components of the middle surface. the strain components are obtained as follows [Mohammadi, Bamdad, Alambaigi et al. (2019c)].

$$\begin{cases} \varepsilon_x = \dfrac{\partial u_x}{\partial x} = \dfrac{\partial u}{\partial x} + z\dfrac{\partial \varphi_x}{\partial x} \\ \varepsilon_z = \dfrac{\partial w_z}{\partial z} = \varphi_z \\ \varepsilon_t = \dfrac{w_z}{r} = \dfrac{w + z\varphi_z}{R + z} \\ \gamma_{xz} = 2 \times \varepsilon_{xz} = \dfrac{\partial u_x}{\partial z} + \dfrac{\partial w_z}{\partial x} = \varphi_x + \dfrac{\partial w}{\partial x} + z\dfrac{\partial \varphi_z}{\partial x} \end{cases} \tag{11}$$

Fig. 3 shows some necessary parameters of the problem.

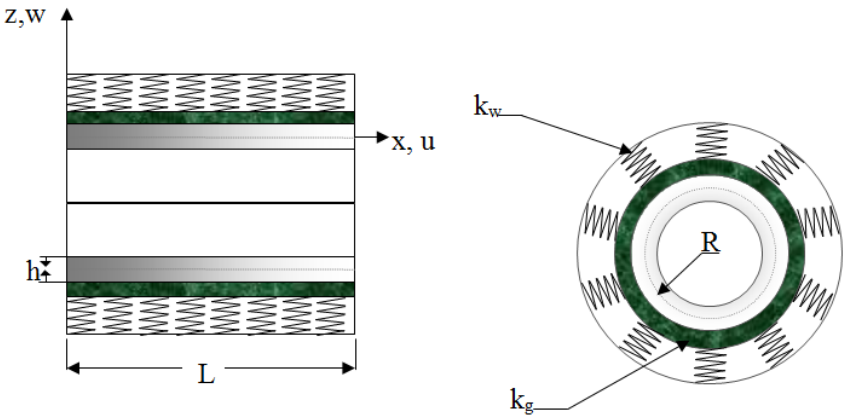

Figure 3: The schematic of a cylindrical pressure vessel resting on Pasternak's foundation

The stress components of each can be obtained from the stress-strain relationship

$$\begin{bmatrix}\sigma_x\\ \sigma_t\\ \sigma_z\\ \tau_{xt}\\ \tau_{xz}\\ \tau_{tz}\end{bmatrix}=\begin{bmatrix}Q_{11} & Q_{12} & Q_{13} & 0 & 0 & 0\\ Q_{21} & Q_{22} & Q_{23} & 0 & 0 & 0\\ Q_{31} & Q_{32} & Q_{33} & 0 & 0 & 0\\ 0 & 0 & 0 & Q_{44} & 0 & 0\\ 0 & 0 & 0 & 0 & Q_{55} & 0\\ 0 & 0 & 0 & 0 & 0 & Q_{66}\end{bmatrix}\begin{bmatrix}\varepsilon_x-\alpha_{11}T\\ \varepsilon_t-\alpha_{22}T\\ \varepsilon_z-\alpha_{33}T\\ \gamma_{xt}\\ \gamma_{xz}\\ \gamma_{tz}\end{bmatrix} \tag{12}$$

where:

$$Q_{11}=\frac{E_{11}}{\Delta}(1-\nu_{23}\nu_{32})\ ,\ Q_{22}=\frac{E_{22}}{\Delta}(1-\nu_{13}\nu_{31})\ ,$$

$$Q_{33}=\frac{E_{33}}{\Delta}(1-\nu_{21}\nu_{12})$$

$$Q_{44}=G_{23}\ ,\ Q_{55}=G_{13}\ ,\ Q_{66}=G_{12} \tag{13}$$

$$Q_{12}=\frac{E_{11}}{\Delta}(\nu_{21}+\nu_{31}\nu_{23})\ ,\ Q_{13}=\frac{E_{11}}{\Delta}(\nu_{31}+\nu_{21}\nu_{32})$$

$$Q_{23}=\frac{E_{22}}{\Delta}(\nu_{32}+\nu_{12}\nu_{31})$$

$$\Delta=1-\nu_{12}\nu_{21}-\nu_{23}\nu_{32}-\nu_{31}\nu_{13}-2\nu_{12}\nu_{32}\nu_{13}$$

3.2 Fundamental equations

Hamilton's principle leads us to the governing equations of motion [Al-Ajmi and Benjeddou (2011); Lee, Lin and Chang (2016)].

$$\delta\Pi=\delta T-\delta U+\delta W=0 \tag{14}$$

δU, δW and δT are the variation of strain energy, virtual work and kinematic energy, respectively and can be defined as follows.

$$\delta U = \int \sigma_{ij} \delta \varepsilon_{ij} d\forall = \int [\sigma_x \delta \varepsilon_x + \sigma_t \delta \varepsilon_t + \sigma_z \delta \varepsilon_z + \tau_{xz} \delta \gamma_{xz}] d\forall \tag{15}$$

$$\delta W = \int \left[P_i \delta w_z|_{z=-\frac{h}{2}} - F_f \delta w_z|_{z=\frac{h}{2}} \right] dA \tag{16}$$

where P_i is the internal pressure and F_f is reaction of Pasternak's foundation. In addition, the other parameters are defined as:

$$\begin{cases} F_f = k_1 \left(w_{z=\frac{h}{2}} \right) - k_2 \dfrac{\partial^2}{\partial x^2} \left(w_{z=\frac{h}{2}} \right) \\ w_{z=\frac{h}{2}} = w + \dfrac{h}{2} \varphi_z \overset{\delta}{\Rightarrow} \delta w + \dfrac{h}{2} \delta \varphi_z \\ \dfrac{\partial^2}{\partial x^2} \left(w_{z=\frac{h}{2}} \right) = \dfrac{\partial^2 w}{\partial x^2} + \dfrac{h}{2} \dfrac{\partial^2 \varphi_z}{\partial x^2} \overset{\delta}{\Rightarrow} \dfrac{\partial^2 \delta w}{\partial x^2} + \dfrac{h}{2} \dfrac{\partial^2 \delta \varphi_z}{\partial x^2} \end{cases} \tag{17}$$

$$F_f = k_1 \left(w + \frac{h}{2} \varphi_z \right) - k_2 \left[\frac{\partial^2 w}{\partial x^2} + \frac{h}{2} \frac{\partial^2 \varphi_z}{\partial x^2} \right]$$

in which $k_1$and $k_2$are direct and shear parameters ofPasternak foundation.

$$\begin{aligned} &\mathrm{T} = \frac{1}{2} \int \rho (\dot{u}^2 + \dot{v}^2 + \dot{w}^2) d\forall \\ &\rightarrow \delta T = \int \rho \left(\dot{u}_x \, \delta \dot{u}_x + \dot{v}_y \, \delta \dot{v}_y + \dot{w}_z \, \delta \dot{w}_z \right) 2\pi (R + z) dz dx \end{aligned} \tag{18}$$

Substituting Eq. (11) into Eqs. (15)-(18) gives the variation of strain energy, virtual work and kinematic energy as follows.

$$\delta U = \iint \begin{bmatrix} \sigma_x \left\{ \frac{\partial \delta u}{\partial x} + z \frac{\partial \delta \varphi_x}{\partial x} \right\} + \sigma_t \left\{ \frac{1}{R+z} [\delta w + z \delta \varphi_z] \right\} + \sigma_z \{ \delta \varphi_z \} \\ + \tau_{xz} \left\{ \delta \varphi_x + \frac{\partial \delta w}{\partial x} + z \frac{\partial \delta \varphi_z}{\partial x} \right\} \end{bmatrix} 2\pi (R + z) dz dx \tag{19}$$

$$\delta U = 2\pi \int \left[\begin{array}{c} \underbrace{\left\{\int \sigma_x (R+z)dz\right\}}_{N_x} \frac{\partial \delta u}{\partial x} + \underbrace{\left\{\int \sigma_x z(R+z)dz\right\}}_{M_x} \frac{\partial \delta \varphi_x}{\partial x} + \\ \underbrace{\left\{\int \sigma_t dz\right\}}_{Q_t} \delta w + \underbrace{\left\{\int \sigma_t z dz\right\}}_{N_t} \delta \varphi_z + \underbrace{\left\{\int \sigma_z (R+z)dz\right\}}_{N_z} \delta \varphi_z + \\ \underbrace{\left\{\int \tau_{xz}(R+z)dz\right\}}_{N_{xz}} \delta \varphi_x + \underbrace{\left\{\int \tau_{xz}(R+z)dz\right\}}_{N_{xz}} \frac{\partial \delta w}{\partial x} + \underbrace{\{\int \tau_{xz} z(R+z)dz\}}_{\Gamma} \frac{\partial \delta \varphi_z}{\partial x} \end{array} \right] dx$$

$$\delta U = 2\pi \int \left[\begin{array}{c} N_x \frac{\partial \delta u}{\partial x} + M_x \frac{\partial \delta \varphi_x}{\partial x} + Q_t \delta w + N_t \delta \varphi_z + N_z \delta \varphi_z + \\ N_{xz} \delta \varphi_x + N_{xz} \frac{\partial \delta w}{\partial x} + \Gamma \frac{\partial \delta \varphi_z}{\partial x} \end{array} \right] dx$$

$$\delta U = 2\pi \int \left[\begin{array}{c} \underbrace{\frac{\partial}{\partial x}(N_x \delta u)}_{0} - \frac{\partial N_x}{\partial x} \delta u + \underbrace{\frac{\partial}{\partial x}(M_x \delta \varphi_x)}_{0} - \\ \frac{\partial M_x}{\partial x} \delta \varphi_x + Q_t \delta w + N_t \delta \varphi_z + N_z \delta \varphi_z + N_{xz} \delta \varphi_x + \\ \underbrace{\frac{\partial}{\partial x}(N_{xz} \delta w)}_{0} - \frac{\partial N_{xz}}{\partial x} \delta w + \underbrace{\frac{\partial}{\partial x}(\Gamma \delta \varphi_z)}_{0} - \frac{\partial \Gamma}{\partial x} \delta \varphi_z \end{array} \right] dx$$

$$\delta U = 2\pi \int \left[\begin{array}{c} -\frac{\partial N_x}{\partial x} \delta u - \frac{\partial M_x}{\partial x} \delta \varphi_x + Q_t \delta w + N_t \delta \varphi_z + \\ N_z \delta \varphi_z + N_{xz} \delta \varphi_x - \frac{\partial N_{xz}}{\partial x} \delta w - \frac{\partial \Gamma}{\partial x} \delta \varphi_z \end{array} \right] dx$$

$$\delta U = 2\pi \int \left[\begin{array}{l} -\frac{\partial N_x}{\partial x} \delta u + (N_{xz} - \frac{\partial M_x}{\partial x}) \delta \varphi_x + (Q_t - \frac{\partial N_{xz}}{\partial x}) \delta w + (N_t + N_z \\ \qquad - \frac{\partial \Gamma}{\partial x}) \delta \varphi_z \end{array} \right] dx$$

$$\delta W = \int \left[P_i \left[\delta w - \frac{h}{2} \delta \varphi_z \right] - F_f \left[\delta w + \frac{h}{2} \delta \varphi_z \right] \right] dA$$

$$= 2\pi \int \left[P_i \underbrace{\left(R - \frac{h}{2} \right)}_{r_i} \left[\delta w - \frac{h}{2} \delta \varphi_z \right] - F_f \underbrace{\left(R + \frac{h}{2} \right)}_{r_o} \left[\delta w + \frac{h}{2} \delta \varphi_z \right] \right] dx \tag{20}$$

$$= 2\pi \int \left[P_i \left(R - \frac{h}{2} \right) \delta w - P_i \left(R - \frac{h}{2} \right) \frac{h}{2} \delta \varphi_z - F_f \left(R + \frac{h}{2} \right) \delta w \right.$$
$$\left. - F_f \left(R + \frac{h}{2} \right) \frac{h}{2} \delta \varphi_z \right] dx$$

$$= 2\pi \int \left[\left\{ P_i\left(R-\frac{h}{2}\right) - F_f\left(R+\frac{h}{2}\right) \right\} \delta w - \left\{ P_i\left(R-\frac{h}{2}\right) + F_f\left(R+\frac{h}{2}\right) \right\} \frac{h}{2} \delta\varphi_z \right] dx$$

$$= 2\pi \int \left[\underbrace{\left\{ P_i\left(R-\frac{h}{2}\right) - \left(k_1\left(w+\frac{h}{2}\varphi_z\right) - k_2\left[\frac{\partial^2 w}{\partial x^2} + \frac{h}{2}\frac{\partial^2 \varphi_z}{\partial x^2}\right]\right)\left(R+\frac{h}{2}\right) \right\}}_{W1} \delta \right.$$

$$\left. - \underbrace{\left\{ \left\{ P_i\left(R-\frac{h}{2}\right) + \left(k_1\left(w+\frac{h}{2}\varphi_z\right) - k_2\left[\frac{\partial^2 w}{\partial x^2} + \frac{h}{2}\frac{\partial^2 \varphi_z}{\partial x^2}\right]\right)\left(R+\frac{h}{2}\right) \right\} \frac{h}{2} \right.}_{W2} \right]$$

$$\delta T = 2\pi \int \left((\dot{u} + z\dot{\varphi}_x)\delta(\dot{u} + z\dot{\varphi}_x) + (\dot{w} + z\dot{\varphi}_z)\delta(\dot{w} + z\dot{\varphi}_z) \right) \rho(R+z) dz dx$$

$$= 2\pi \int \left[\begin{pmatrix} \dot{u}\delta\dot{u} + \dot{u}z\delta\dot{\varphi}_x + z\dot{\varphi}_x\delta\dot{u} + z^2\dot{\varphi}_x\delta\dot{\varphi}_x + \dot{w}\delta\dot{w} + \\ \dot{w}z\delta\dot{\varphi}_z + z\dot{\varphi}_z\delta\dot{w} + z^2\dot{\varphi}_z\delta\dot{\varphi}_z \end{pmatrix} \rho(R+z) \right] dz dx$$

$$= 2\pi \int \left[\left(\begin{array}{c} \left\{ \underbrace{\dot{u}\rho(R+z)dz}_{I_1} \right\} \delta\dot{u} + \left\{ \underbrace{\dot{u}z\rho(R+z)dz}_{I_2} \right\} \delta\dot{\varphi}_x + \left\{ \underbrace{z\rho\dot{\varphi}_x(R+z)dz}_{I_3} \right\} \delta\dot{u} + \\ \left\{ \underbrace{z^2\dot{\varphi}_x\rho(R+z)dz}_{I_4} \right\} \delta\dot{\varphi}_x + \left\{ \underbrace{\dot{w}\rho(R+z)dz}_{I_5} \right\} \delta\dot{w} + \\ \left\{ \underbrace{\dot{w}z\rho(R+z)dz}_{I_6} \right\} \delta\dot{\varphi}_z + \left\{ \underbrace{z\dot{\varphi}_z\rho(R+z)dz}_{I_7} \right\} \delta\dot{w} + \left\{ \underbrace{z^2\rho\dot{\varphi}_z(R+z)dz}_{I_8} \right\} \delta\dot{\varphi}_z \end{array} \right) \right] \quad (21)$$

$$= 2\pi \int \left[(I_1\delta\dot{u} + I_2\delta\dot{\varphi}_x + I_3\delta\dot{u} + I_4\delta\dot{\varphi}_x + I_5\delta\dot{w} + I_6\delta\dot{\varphi}_z + I_7\delta\dot{w} + I_8\delta\dot{\varphi}_z) \right] dx$$

$$= 2\pi \int \left[\left(-\dot{I}_1\delta u - \dot{I}_2\delta\varphi_x - \dot{I}_3\delta u - \dot{I}_4\delta\varphi_x - \dot{I}_5\delta w - \dot{I}_6\delta\varphi_z - \dot{I}_7\delta w - \dot{I}_8\delta\varphi_z \right) \right] dx$$

$$= 2\pi \int \left[(-\dot{I}_1 - \dot{I}_3)\delta u + (-\dot{I}_2 - \dot{I}_4)\delta\varphi_x + (-\dot{I}_5 - \dot{I}_7)\delta w + (-\dot{I}_6 - \dot{I}_8)\delta\varphi_z \right] dx$$

Substituting Eqs. (19-21) into Eq. (14) leads to:

$$\delta\Pi = 2\pi \int \left[\begin{array}{c} \left(\frac{\partial N_x}{\partial x} - \left(\dot{I}_1 + \dot{I}_3\right) \right) \delta u - \left(N_{xz} - \frac{\partial M_x}{\partial x} + \left(\dot{I}_2 + \dot{I}_4\right) \right) \delta\varphi_x - \\ \left(Q_t - \frac{\partial N_{xz}}{\partial x} + \left(\dot{I}_5 + \dot{I}_7\right) - W1 \right) \delta w - \\ \left(N_t + N_z - \frac{\partial \Gamma}{\partial x} + \left(\dot{I}_6 + \dot{I}_8\right) + W2 \right) \delta\varphi_z \end{array} \right] dx = 0 \quad (22)$$

And four fundamental equations are derived as:

$$\begin{cases} \delta u: \dfrac{\partial N_x}{\partial x} - \left(\dot{I}_1 + \dot{I}_3\right) = 0 \\ \delta \varphi_x: N_{xz} - \dfrac{\partial M_x}{\partial x} + \left(\dot{I}_2 + \dot{I}_4\right) = 0 \\ \delta w: Q_t - \dfrac{\partial N_{xz}}{\partial x} + \left(\dot{I}_5 + \dot{I}_7\right) - W1 = 0 \\ \delta \varphi_z: N_t + N_z - \dfrac{\partial \Gamma}{\partial x} + \left(\dot{I}_6 + \dot{I}_8\right) + W2 = 0 \end{cases} \tag{23}$$

Using Eqs. (23) and (12) results in four extended equations which have beenpresented in Appendix.

The next step of solution procedure is choosing equations which can satisfy boundary conditions. As our aim is investigation on different boundary conditions, specific equations are proposed as following equations and Tab. 1.

$$\begin{aligned} u &= \sum_{m=1}^{\infty}\sum_{n=1}^{\infty} U_{mn}\frac{\partial X_m(x)}{\partial x}e^{iw_n t} \\ \varphi_x &= \sum_{m=1}^{\infty}\sum_{n=1}^{\infty} \phi_x\frac{\partial X_m(x)}{\partial x}e^{iw_n t} \\ w &= \sum_{m=1}^{\infty}\sum_{n=1}^{\infty} W_{mn}X_m(x)e^{iw_n t} \\ \varphi_z &= \sum_{m=1}^{\infty}\sum_{n=1}^{\infty} \phi_z X_m(x)e^{iw_n t} \end{aligned} \tag{24}$$

Table1: The admissible function $X_m(x)$ for different boundary conditions

	Boundary conditions At $x = 0, L$	$X_m(x)$
Simply-Simply	$X_m(0) = X_m''(0) = 0$ $X_m(L) = X_m''(L) = 0$	$Sin(Lx)$
Clamped-Simply	$X_m(0) = X_m'(0) = 0$ $X_m(L) = X_m''(L) = 0$	$Sin(Lx)[Cos(Lx) - 1]$
Clamped-Clamped	$X_m(0) = X_m'(0) = 0$ $X_m(L) = X_m'(L) = 0$	$Sin^2(Lx)$
Clamped-Free	$X_m(0) = X_m'''(0) = 0$ $X_m(L) = X_m'''(L) = 0$	$Cos^2(Lx)[Sin^2(Lx) + 1]$

Substituting Eq. (24) into equations, which have been presented in Appendix, leads to an equation as:

$$[M]\{\ddot{\omega}\} + [A]\{\omega\} = 0 \tag{25}$$

where

$$\{\omega\} = \begin{Bmatrix} U_{mn} \\ \phi_x \\ W_{mn} \\ \phi_z \end{Bmatrix}$$

The natural frequencies can be obtained from the Eq. (25).

4 Numerical results and discussion

In this section, effects offour parameters including CNT distribution patterns, CNT volume fractions, boundary conditions and Pasternak's coefficients on the natural frequency are investigated.

4.1Patterns effects

Shown in Fig. 4 is variation of fundamental natural frequencies of FG-CNTRC cylindrical shell in terms of length to thickness ratio L/h for various distributions of reinforcement (UD, FG-X and FG-V). The numerical results show that with increase of length to thickness ratio (L/h), the fundamental natural frequenciesdecrease significantly. It can be concluded that this decrease is due to decrease of stiffness of cylindrical shell. In addition, this investigation shows that the highest values are obtained for FG-X distribution while the lowest one is obtained for U-D.

Behaviors of second and third natural frequencies of FG-CNTRC cylindrical shell in terms of length to thickness ratio (L/h) for various distributions of reinforcement (UD, FG-X and FG-V) are presented in Figs. 5 and 6, respectively. The same conclusions for Fig. 4 can be expressed for Figs. 5 and 6.

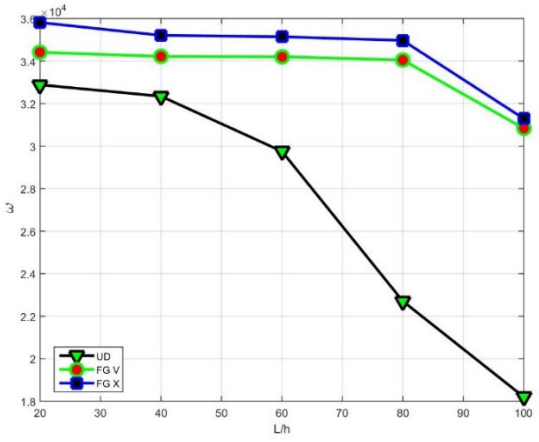

Figure 4: Fundamental natural frequencies in terms of L/h for various distributions of reinforcement

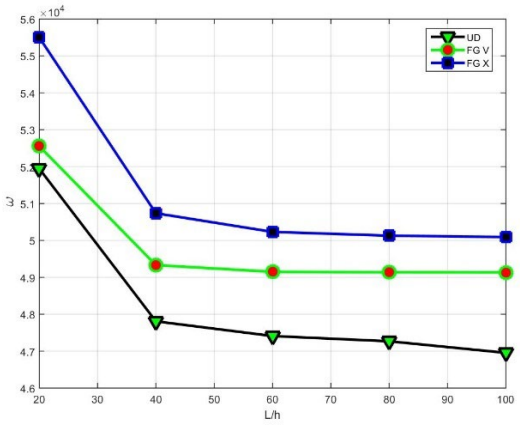

Figure 5: Second natural frequencies in terms of L/h for various distributions of reinforcement

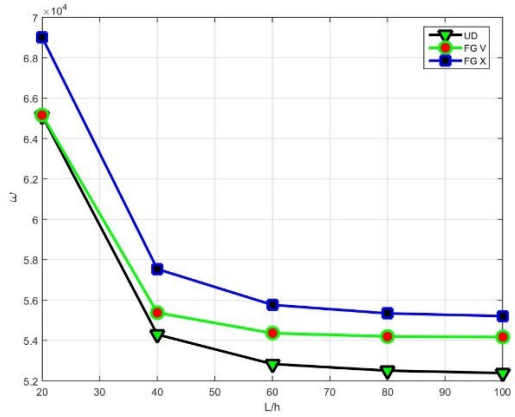

Figure 6: Third natural frequencies in terms of L/h for various distributions of reinforcement

4.2 Boundary conditions effects

This section ispresented to investigate the influence of various boundary conditions on the free vibration responses of FG-CNTRC cylindrical shell. Shown in Fig. 7 is variation of fundamental natural frequencies of FG-CNTRC cylindrical shell in terms of length to thickness ratio (L/h) for various boundary conditions (simply-simply, clamped-simply, clamped-clamped).The numerical results indicate in addition to corresponding increase of natural frequencies due to increase in L/h ratio, the highest values of natural frequencies are reachedby CC boundary conditions while the lowest one is obtained for SS boundary conditions. Figs. 8 and 9 show variation of second and third natural frequencies of FG-CNTRC cylindrical shell in terms of length to thickness ratio (L/h) for various boundary conditions (SS, CS, CC).

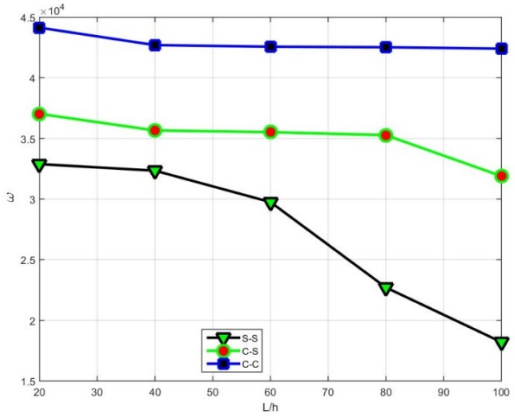

Figure 7: Fundamental natural frequencies in terms of L/h for various boundary conditions

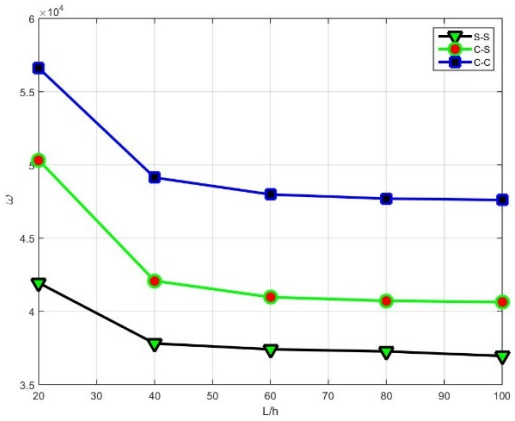

Figure 8: Second natural frequencies in terms of L/h for various boundary conditions

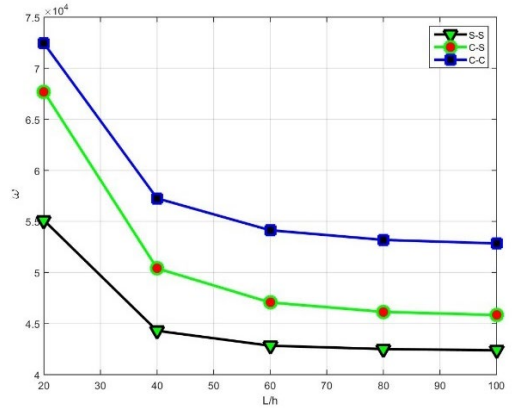

Figure 9: Third natural frequencies in terms of L/h for various boundary conditions

4.3 CNTs volume fractions effects

In this section, the influence of various CNTs volume fractions of reinforcement on the natural frequencies of FG-CNTRCs cylindrical pressure vessels is investigated. Shown in Fig. 10 is variation of fundamental natural frequencies of FG-CNTRC cylindrical pressure vessels in terms of length to thickness ratio (L/h) for various volume fractions of carbon nanotube reinforcement. The numerical results indicate that the natural frequencies increase significantly with increase of volume fraction of carbon nanotube reinforcement (0.12, 0.17 and 0.28). One can be concluded that with increase of volume fractions of carbon nanotube reinforcement, the stiffness of FG-CNTRCs cylindrical pressure vesselsincreases and consequently the natural frequency increases significantly. Shown in Figs. 11 and 12 are variation of second and third natural frequencies of FG-CNTRC cylindrical pressure vesselsin terms of length to thickness ratio (L/h) for various volume fractions of carbon nanotube reinforcement.

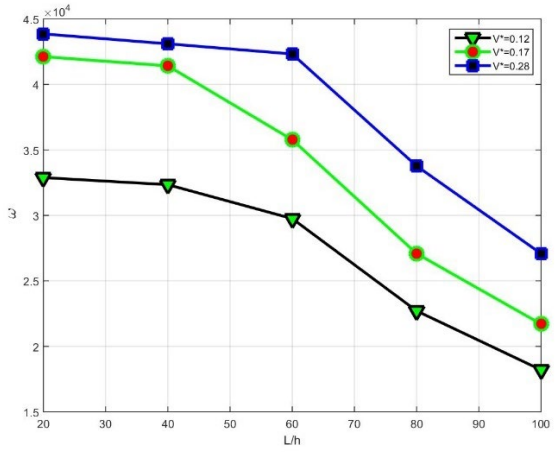

Figure 10: Fundamental natural frequency in terms of L/h for various volume fractions of CNT

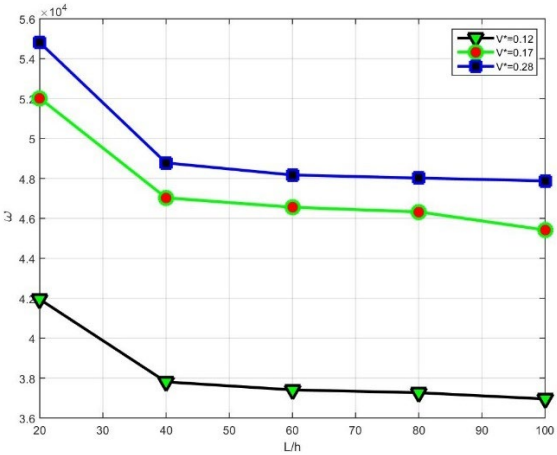

Figure 11: Second natural frequency in terms of L/h for various volume fractions of CNT

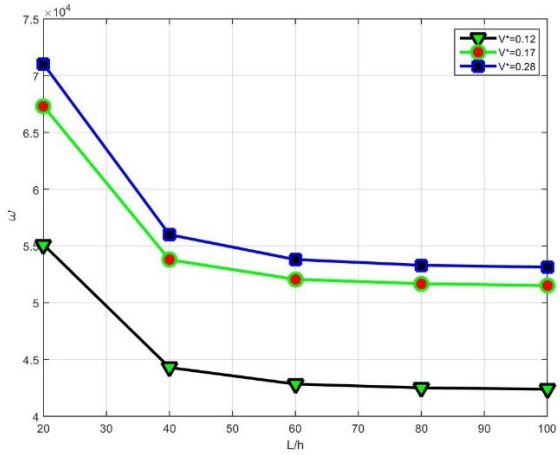

Figure 12: Third natural frequency in terms of L/h for various volume fractions of CNT

4.4 Pasternak's coefficients effects

Fig. 13 shows variation of fundamental natural frequencies of FG-CNTRC cylindrical pressure vessels in terms of two parameters of Pasternak's foundation. The numerical results indicate that increase in Pasternak's parametersincreases the stiffness of the foundation, and increases the natural frequency.

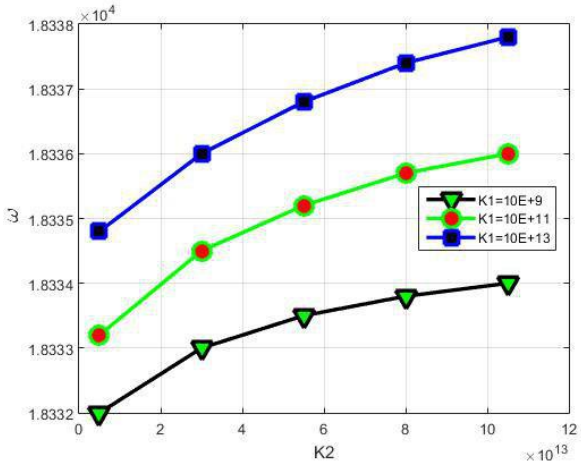

Figure 13: The effects of the K_1 and K_2 on the fundamental natural frequencies of the FG-CNTRC cylindrical pressure vessels

5 Conclusion

Free vibration characteristics of FG-CNTRC cylindrical pressure vessels with various boundary conditions were investigated in this paper based on Hamilton's principle and first-order shear deformation theory. Rule of mixture was used to calculate the effective material properties of reinforced structure.The influences of various important parameters

of the problem such as various boundary conditions, various volume fractions of reinforcement, length to thickness ratio (L/h), and two parameters of Pasternak's foundation were studied.

Investigation on the influence of length to thickness ratio (L/h) indicates that with increase of this dimensionless parameter, all natural frequencies of FG-CNTRC cylindrical pressure vessels decrease significantly. One can be concluded that with increase of this dimensionless parameter, the stiffness of reinforced structure decreases and consequently the natural frequencies decrease significantly.

The influence of various patterns (UD, FG-X and FG-V) was studied on the natural frequencies of cylindrical pressure vessel. The numerical results indicate that FG-X distribution has higher stiffness that leads to highest natural frequencies. In addition, the lowest natural frequencies are obtained for UD. Increasing of volume fraction of reinforcement increases the stiffness of cylindrical shellthat leads to increase the natural frequencies.

The influence of Pasternak's parameters was studied on the free vibration characteristics of FG-CNTRC cylindrical pressure vessels. The numerical results indicate that increase of Pasternak's parameters leads to increase the natural frequencies.

Acknowledgment: This work was financially supported by the University of Kashan (Grant Number: 574613/026). M. Arefi would like to thank the Iranian Nanotechnology Development Committee for their financial support.

Conflicts of Interest: The authors declare that they have no conflicts of interest to report regarding the present study.

References

Akgöz, B.; Civalek, Ö. (2017): Effects of thermal and shear deformation on vibration response of functionally graded thick composite microbeams. *Composites Part B: Engineering*, vol. 129, pp. 77-87.

Al-Ajmi, M.; Benjeddou, A. (2011): A new discrete-layer finite element for electromechanically coupled analyses of piezoelectric adaptive composite structures. *Computers, Materials and Continua*, vol. 23, no. 3, pp. 265-285.

Arefi, M.; Zenkour, A. M. (2016): Free vibration, wave propagation and tension analyses of a sandwich micro/nano rod subjected to electric potential using strain gradient theory. *Materials Research Express*, vol. 3, no. 11.

Asadi, H.; Souri, M.; Wang, Q. (2017): A numerical study on flow-induced instabilities of supersonic FG-CNT reinforced composite flat panels in thermal environments. *Composite Structures*, vol. 171, pp. 113-125.

Feng, C.; Kitipornchai, S.; Yang, J. (2017): Nonlinear free vibration of functionally graded polymer composite beams reinforced with graphene nanoplatelets (GPLs). *Engineering Structures*, vol. 140, pp. 110-119.

Kalnins, K.; Wieder, A. (2017): Test results on the stability and vibrations of composite

shells. *Stability and Vibrations of Thin Walled Composite Structures*, pp. 619-691.

Kiani, Y. (2016): Free vibration of FG-CNT reinforced composite skew plates. *Aerospace Science and Technology*, vol. 58, pp. 178-188.

Lee, S. Y.; Lin, S. M.; Chang, K. P. (2016): Exact solutions and mode transition for out-of-plane vibrations of non-uniform beams with variable curvature. *Computers, Materials & Continua*, vol. 51, no. 1, pp. 1-19.

Miao, Y.; Chen, Z.; Wang, Q.; Zhu, H. P. (2014): Mechanical analysis of 3D composite materials by hybrid boundary node method. *Computers, Materials & Continua*, vol. 43, no. 1, pp. 49-73.

Mirzaei, M.; Kiani, Y. (2016): Free vibration of functionally graded carbon nanotube reinforced composite cylindrical panels. *Composite Structures*, vol. 142, pp. 45-56.

Mohammadi, M.; Bamdad, M.; Alambeigi, K.; Dimitri, R.; Tornabene, F. (2019c): Electro-elastic response of cylindrical sandwich pressure vessels with porous core and piezoelectric face-sheets. *Composite Structures*, vol. 225, 111119

SafarPour, H.; Ghanbari, B.; Ghadiri, M. (2019): Buckling and free vibration analysis of high speed rotating carbon nanotube reinforced cylindrical piezoelectric shell. *Applied Mathematical Modelling*, vol. 65, pp. 428-442.

Sayyad, A. S.; Ghugal, Y. M. (2017): Bending, buckling and free vibration of laminated composite and sandwich beams: a critical review of literature. *Composite Structures*, vol. 171, pp. 486-504.

Tan, P.; Nguyen-Thanh, N.; Rabczuk, T.; Zhou, K. (2018): Static, dynamic and buckling analyses of 3D FGM plates and shells via an isogeometric-meshfree coupling approach. *Composite Structures*, vol. 198, pp. 35-50.

Zhao, J.; Choe, K.; Shuai, C.; Wang, A.; Wang, Q. (2019): Free vibration analysis of laminated composite elliptic cylinders with general boundary conditions. *Composites Part B: Engineering*, vol. 158, pp. 55-66.

Appendix

$$\delta u: \frac{\partial N_x}{\partial x} - \left(\dot{I}_1 + \dot{I}_3\right) = 0$$

$$\rightarrow \frac{\partial}{\partial x}\int (\sigma_x(R+z) - (\ddot{u}\rho(R+z)dz + z\rho\ddot{\varphi}_x(R+z))dz) = 0$$

$$\rightarrow \frac{\partial}{\partial x}\int \begin{pmatrix} Q_{11}\varepsilon_x - Q_{11}\alpha_{11}T + Q_{12}\varepsilon_t - Q_{12}\alpha_{22}T + \\ Q_{13}\varepsilon_z - Q_{13}\alpha_{33}T \end{pmatrix}(R+z)dz -$$

$$\int (\ddot{u}\rho(R+z)dz \; + z\rho\dot{\varphi}_x(R+z)dz) = 0$$

$$\rightarrow \frac{\partial}{\partial x}\int \begin{bmatrix} Q_{11}\left(\frac{\partial u}{\partial x} + z\frac{\partial \varphi_x}{\partial x}\right) - Q_{11}\alpha_{11}T + \\ Q_{12}\left(\frac{w + z\varphi_z}{R+z}\right) - Q_{12}\alpha_{22}T + \\ Q_{13}\varphi_z - Q_{13}\alpha_{33}T \end{bmatrix}(R+z)dz - \int \ddot{u}\rho(R+z)dz$$

$$- \int z\rho\ddot{\varphi}_x(R+z)dz = 0$$

$$\rightarrow \int \begin{bmatrix} Q_{11}\left(\frac{\partial^2 u}{\partial x^2} + z\frac{\partial^2 \varphi_x}{\partial x^2}\right)R + Q_{12}\left(\frac{\left(\frac{\partial w}{\partial x} + z\frac{\partial \varphi_z}{\partial x}\right)}{R+z}\right)R + \\ Q_{13}R\frac{\partial \varphi_z}{\partial x} + \\ Q_{11}\left(\frac{\partial^2 u}{\partial x^2} + z\frac{\partial^2 \varphi_x}{\partial x^2}\right)z + Q_{12}\left(\frac{\left(\frac{\partial w}{\partial x} + z\frac{\partial \varphi_z}{\partial x}\right)}{R+z}\right)z + \\ Q_{13}z\frac{\partial \varphi_z}{\partial x} \end{bmatrix} dz -$$

$$\int \ddot{u}\rho(R+z)dz - \int z\rho\ddot{\varphi}_x(R+z)dz = 0$$

$$\rightarrow \int \begin{bmatrix} Q_{11}R\dfrac{\partial^2 u}{\partial x^2} + Q_{11}zR\dfrac{\partial^2 \varphi_x}{\partial x^2} + \dfrac{Q_{12}R}{R+z}\dfrac{\partial w}{\partial x} + \\ \dfrac{Q_{12}Rz}{R+z}\dfrac{\partial \varphi_z}{\partial x} + Q_{13}R\dfrac{\partial \varphi_z}{\partial x} + \\ Q_{11}z\dfrac{\partial^2 u}{\partial x^2} + Q_{11}z^2\dfrac{\partial^2 \varphi_x}{\partial x^2} + \dfrac{Q_{12}z}{R+z}\dfrac{\partial w}{\partial x} + \\ \dfrac{Q_{12}z^2}{R+z}\dfrac{\partial \varphi_z}{\partial x} + Q_{13}z\dfrac{\partial \varphi_z}{\partial x} \end{bmatrix} dz - \int \ddot{u}\rho(R+z)dz$$

$$- \int z\rho\ddot{\varphi}_x(R+z)dz = 0$$

$$\rightarrow \delta u : R\frac{\partial^2 u}{\partial x^2}\int Q_{11}dz + R\frac{\partial^2 \varphi_x}{\partial x^2}\int Q_{11}zdz + R\frac{\partial w}{\partial x}\int \frac{Q_{12}}{R+z}dz + R\frac{\partial \varphi_z}{\partial x}\int \frac{Q_{12}z}{R+z}dz +$$

$$R\frac{\partial \varphi_z}{\partial x}\int Q_{13}dz + \frac{\partial^2 u}{\partial x^2}\int Q_{11}zdz + \frac{\partial^2 \varphi_x}{\partial x^2}\int Q_{11}z^2dz + \frac{\partial w}{\partial x}\int \frac{Q_{12}z}{R+z}dz$$

$$+ \frac{\partial \varphi_z}{\partial x}\int \frac{Q_{12}z^2}{R+z}dz +$$

$$\frac{\partial \varphi_z}{\partial x}\int Q_{13}zdz - \ddot{u}R\int \rho dz - \ddot{u}\int \rho z dz - \ddot{\varphi}_x R\int z\rho dz - \ddot{\varphi}_x \int z^2\rho dz = 0$$

$$\delta\varphi_x : N_{xz} - \frac{\partial M_x}{\partial x} + \left(\dot{I}_2 + \dot{I}_4\right) = 0$$

$$\rightarrow \int Q_{55}\left(\varphi_x + \frac{\partial w}{\partial x} + z\frac{\partial \varphi_z}{\partial x}\right)Rdz + \int Q_{55}\left(\varphi_x + \frac{\partial w}{\partial x} + z\frac{\partial \varphi_z}{\partial x}\right)zdz -$$

$$\int \begin{bmatrix} Q_{11}Rz\dfrac{\partial^2 u}{\partial x^2} + Q_{11}z^2R\dfrac{\partial^2 \varphi_x}{\partial x^2} + \dfrac{Q_{12}Rz}{R+z}\dfrac{\partial w}{\partial x} + \\ \dfrac{Q_{12}Rz^2}{R+z}\dfrac{\partial \varphi_z}{\partial x} + Q_{13}Rz\dfrac{\partial \varphi_z}{\partial x} + \\ Q_{11}z^2\dfrac{\partial^2 u}{\partial x^2} + Q_{11}z^3\dfrac{\partial^2 \varphi_x}{\partial x^2} + \dfrac{Q_{12}z^2}{R+z}\dfrac{\partial w}{\partial x} + \\ \dfrac{Q_{12}z^3}{R+z}\dfrac{\partial \varphi_z}{\partial x} + Q_{13}z^2\dfrac{\partial \varphi_z}{\partial x} \end{bmatrix} dz + \int \ddot{u}z\rho R dz + \int \ddot{u}z^2\rho dz +$$

$$\int z^2\ddot{\varphi}_x\rho R dz + \int z^3\ddot{\varphi}_x\rho dz = 0$$

$$\rightarrow \int Q_{55}\varphi_x R dz + \int Q_{55}\frac{\partial w}{\partial x}Rdz + \int Q_{55}z\frac{\partial \varphi_z}{\partial x}Rdz + \int Q_{55}\varphi_x z dz + \int Q_{55}\frac{\partial w}{\partial x}zdz +$$

$$\int Q_{55}z^2\frac{\partial \varphi_z}{\partial x}dz - \int \begin{bmatrix} Q_{11}Rz\dfrac{\partial^2 u}{\partial x^2} + Q_{11}z^2R\dfrac{\partial^2 \varphi_x}{\partial x^2} + \dfrac{Q_{12}Rz}{R+z}\dfrac{\partial w}{\partial x} + \\ \dfrac{Q_{12}Rz^2}{R+z}\dfrac{\partial \varphi_z}{\partial x} + Q_{13}Rz\dfrac{\partial \varphi_z}{\partial x} + \\ Q_{11}z^2\dfrac{\partial^2 u}{\partial x^2} + Q_{11}z^3\dfrac{\partial^2 \varphi_x}{\partial x^2} + \dfrac{Q_{12}z^2}{R+z}\dfrac{\partial w}{\partial x} + \\ \dfrac{Q_{12}z^3}{R+z}\dfrac{\partial \varphi_z}{\partial x} + Q_{13}z^2\dfrac{\partial \varphi_z}{\partial x} \end{bmatrix} dz + \int \ddot{u}z\rho R dz +$$

$$\int \ddot{u}z^2\rho dz + \int z^2\ddot{\varphi}_x\rho R dz + \int z^3\ddot{\varphi}_x\rho dz = 0$$

$$\rightarrow \delta\varphi_x : \varphi_x R\int Q_{55}dz + \frac{\partial w}{\partial x}R\int Q_{55}dz + \frac{\partial \varphi_z}{\partial x}R\int Q_{55}zdz + \varphi_x\int Q_{55}zdz +$$

$$\frac{\partial w}{\partial x}\int Q_{55}zdz + \frac{\partial \varphi_z}{\partial x}\int Q_{55}z^2dz - R\frac{\partial^2 u}{\partial x^2}\int Q_{11}zdz - R\frac{\partial^2 \varphi_x}{\partial x^2}\int Q_{11}z^2dz -$$

$$R\frac{\partial w}{\partial x}\int \frac{Q_{12}z}{R+z}dz - R\frac{\partial \varphi_z}{\partial x}\int \frac{Q_{12}z^2}{R+z}dz - R\frac{\partial \varphi_z}{\partial x}\int Q_{13}zdz - \frac{\partial^2 u}{\partial x^2}\int Q_{11}z^2dz -$$

$$\frac{\partial^2 \varphi_x}{\partial x^2}\int Q_{11}z^3dz - \frac{\partial w}{\partial x}\int \frac{Q_{12}z^2}{R+z}dz - \frac{\partial \varphi_z}{\partial x}\int \frac{Q_{12}z^3}{R+z}dz - \frac{\partial \varphi_z}{\partial x}\int Q_{13}z^2dz + \ddot{u}R\int z\rho dz$$

$$+$$

$$\ddot{u}\int z^2\rho dz + \ddot{\varphi}_x R\int z^2\rho dz + \ddot{\varphi}_x\int z^3\rho dz = 0$$

$$\delta w : \; Q_t - \frac{\partial N_{xz}}{\partial x} + \left(\dot{I}_5 + \dot{I}_7\right) - W1 = 0$$

$$\rightarrow \int \sigma_t dz - \frac{\partial}{\partial x}\int \tau_{xz}(R+z)dz + \int \ddot{w}\rho(R+z)dz +$$

$$\int z\ddot{\varphi}_z\rho(R+z)dz + 2\pi\left(k_1\left(w + \frac{h}{2}\varphi_z\right) - k_2\left[\frac{\partial^2 w}{\partial x^2} + \frac{h}{2}\frac{\partial^2 \varphi_z}{\partial x^2}\right]\right)\left(R + \frac{h}{2}\right) = 0$$

$$\rightarrow \int (Q_{12}\varepsilon_x - Q_{12}\alpha_{11}T + Q_{22}\varepsilon_t - Q_{22}\alpha_{22}T + Q_{23}\varepsilon_z - Q_{23}\alpha_{33}T)dz -$$

$$\frac{\partial}{\partial x}\int (Q_{55}\gamma_{xz})(R+z)dz + \int \ddot{w}\rho(R+z)dz + \int z\ddot{\varphi}_z\rho(R+z)dz +$$

$$\left(k_1\left(w+\frac{h}{2}\varphi_z\right)-k_2\left[\frac{\partial^2 w}{\partial x^2}+\frac{h}{2}\frac{\partial^2\varphi_z}{\partial x^2}\right]\right)\left(R+\frac{h}{2}\right)=0$$

$$\rightarrow\int\left(Q_{12}\left(\frac{\partial u}{\partial x}+z\frac{\partial\varphi_x}{\partial x}\right)-Q_{12}\alpha_{11}T+Q_{22}\left(\frac{w+z\varphi_z}{R+z}\right)-Q_{22}\alpha_{22}T+Q_{23}\varphi_z - Q_{23}\alpha_{33}T\right)dz -$$

$$\frac{\partial}{\partial x}\int\left(Q_{55}\left(\varphi_x+\frac{\partial w}{\partial x}+z\frac{\partial\varphi_z}{\partial x}\right)\right)(R+z)dz+\int\ddot{w}\rho(R+z)dz+$$

$$\int z\ddot{\varphi}_z\rho(R+z)dz+2\pi\left(k_1\left(w+\frac{h}{2}\varphi_z\right)-k_2\left[\frac{\partial^2 w}{\partial x^2}+\frac{h}{2}\frac{\partial^2\varphi_z}{\partial x^2}\right]\right)\left(R+\frac{h}{2}\right)=0$$

$$\rightarrow\int\left(Q_{12}\frac{\partial u}{\partial x}+Q_{12}z\frac{\partial\varphi_x}{\partial x}-Q_{12}\alpha_{11}T+\frac{Q_{22}}{R+z}w+\frac{Q_{22}z}{R+z}\varphi_z-Q_{22}\alpha_{22}T+Q_{23}\varphi_z - Q_{23}\alpha_{33}T\right)dz -$$

$$\int\left(Q_{55}R\frac{\partial\varphi_x}{\partial x}+Q_{55}R\frac{\partial^2 w}{\partial x^2}+Q_{55}zR\frac{\partial^2\varphi_z}{\partial x^2}+Q_{55}z\frac{\partial\varphi_x}{\partial x}+Q_{55}z\frac{\partial^2 w}{\partial x^2}+Q_{55}z^2\frac{\partial^2\varphi_z}{\partial x^2}\right)dz +$$

$$\int(R\ddot{w}\rho+z\ddot{w}\rho)dz+\int(Rz\ddot{\varphi}_z\rho+z^2\ddot{\varphi}_z\rho)dz+2\pi wk_1R+2\pi\frac{h}{2}Rk_1\varphi_z-2\pi Rk_2\frac{\partial^2 w}{\partial x^2} -$$

$$2\pi Rk_2\frac{h}{2}\frac{\partial^2\varphi_z}{\partial x^2}+2\pi wk_1\frac{h}{2}+\left(\frac{h}{2}\right)^2k_1\varphi_z-2\pi k_2\frac{h}{2}\frac{\partial^2 w}{\partial x^2}-2\pi k_2\left(\frac{h}{2}\right)^2\frac{\partial^2\varphi_z}{\partial x^2}=0$$

$$\rightarrow\delta w:\ \frac{\partial u}{\partial x}\int Q_{12}dz+\frac{\partial\varphi_x}{\partial x}\int Q_{12}zdz-\alpha_{11}T\int Q_{12}dz+w\int\frac{Q_{22}}{R+z}dz + \varphi_z\int\frac{Q_{22}z}{R+z}dz -$$

$$\alpha_{22}T\int Q_{22}dz+\varphi_z\int Q_{23}dz-\alpha_{33}T\int Q_{23}dz-R\frac{\partial\varphi_x}{\partial x}\int Q_{55}dz-R\frac{\partial^2 w}{\partial x^2}\int Q_{55}dz -$$

$$R\frac{\partial^2\varphi_z}{\partial x^2}\int Q_{55}zdz-\frac{\partial\varphi_x}{\partial x}\int Q_{55}zdz-\frac{\partial^2 w}{\partial x^2}\int Q_{55}zdz-\frac{\partial^2\varphi_z}{\partial x^2}\int Q_{55}z^2dz+R\ddot{w}\int\rho dz +$$

$$\ddot{w}\int z\rho dz+R\ddot{\varphi}_z\int z\rho dz+\ddot{\varphi}_z\int z^2\rho dz+2\pi wk_1R+2\pi\frac{h}{2}Rk_1\varphi_z-2\pi Rk_2\frac{\partial^2 w}{\partial x^2} -$$

$$2\pi Rk_2\frac{h}{2}\frac{\partial^2\varphi_z}{\partial x^2}+2\pi wk_1\frac{h}{2}+2\pi\left(\frac{h}{2}\right)^2k_1\varphi_z-2\pi k_2\frac{h}{2}\frac{\partial^2 w}{\partial x^2}-2\pi k_2\left(\frac{h}{2}\right)^2\frac{\partial^2\varphi_z}{\partial x^2}=0$$

$$\delta\varphi_z:\ N_t+N_z-\frac{\partial\Gamma}{\partial x}+\left(\dot{I}_6+\dot{I}_8\right)+W2=0$$

$$\rightarrow \int \sigma_t z dz + \int \sigma_z (R+z) dz - \frac{\partial}{\partial x} \int \tau_{xz} z (R+z) dz + \int \ddot{w} z \rho (R+z) dz + \int z^2 \rho \ddot{\varphi}_z (R+z) dz +$$

$$2\pi R w k_1 \frac{h}{2} + 2\pi R k_1 \varphi_z \left(\frac{h}{2}\right)^2 - 2\pi R k_2 \frac{\partial^2 w}{\partial x^2} \frac{h}{2} - 2\pi R k_2 \frac{\partial^2 \varphi_z}{\partial x^2} \left(\frac{h}{2}\right)^2 + 2\pi w k_1 \left(\frac{h}{2}\right)^2 +$$

$$2\pi k_1 \varphi_z \left(\frac{h}{2}\right)^3 - 2\pi k_2 \frac{\partial^2 w}{\partial x^2} \left(\frac{h}{2}\right)^2 - 2\pi k_2 \frac{\partial^2 \varphi_z}{\partial x^2} \left(\frac{h}{2}\right)^3 = 0$$

$$\rightarrow \int (Q_{12}\varepsilon_x - Q_{12}\alpha_{11}T + Q_{22}\varepsilon_t - Q_{22}\alpha_{22}T + Q_{23}\varepsilon_z - Q_{23}\alpha_{33}T) z dz +$$

$$\int (Q_{13}\varepsilon_x - Q_{13}\alpha_{11}T + Q_{23}\varepsilon_t - Q_{23}\alpha_{22}T + Q_{33}\varepsilon_z - Q_{33}\alpha_{33}T)(R+z) dz -$$

$$\frac{\partial}{\partial x} \int (Q_{55}\gamma_{xz}) z (R+z) dz + \int \ddot{w} z \rho (R+z) dz + \int z^2 \rho \ddot{\varphi}_z (R+z) dz + 2\pi R w k_1 \frac{h}{2} +$$

$$2\pi R k_1 \varphi_z \left(\frac{h}{2}\right)^2 - 2\pi R k_2 \frac{\partial^2 w}{\partial x^2} \frac{h}{2} - 2\pi R k_2 \frac{\partial^2 \varphi_z}{\partial x^2} \left(\frac{h}{2}\right)^2 + 2\pi w k_1 \left(\frac{h}{2}\right)^2 +$$

$$2\pi k_1 \varphi_z \left(\frac{h}{2}\right)^3 - 2\pi k_2 \frac{\partial^2 w}{\partial x^2} \left(\frac{h}{2}\right)^2 - 2\pi k_2 \frac{\partial^2 \varphi_z}{\partial x^2} \left(\frac{h}{2}\right)^3 = 0$$

$$\rightarrow \int \left(Q_{12}\left(\frac{\partial u}{\partial x} + z\frac{\partial \varphi_x}{\partial x}\right) - Q_{12}\alpha_{11}T + Q_{22}\left(\frac{w + z\varphi_z}{R+z}\right) - Q_{22}\alpha_{22}T + Q_{23}\varphi_z - Q_{23}\alpha_{33}T\right) z dz +$$

$$\int \left(Q_{13}\left(\frac{\partial u}{\partial x} + z\frac{\partial \varphi_x}{\partial x}\right) - Q_{13}\alpha_{11}T + Q_{23}\left(\frac{w + z\varphi_z}{R+z}\right) - Q_{23}\alpha_{22}T + Q_{33}\varphi_z - Q_{33}\alpha_{33}T\right)(R+z) dz -$$

$$\frac{\partial}{\partial x} \int \left(Q_{55}\left(\varphi_x + \frac{\partial w}{\partial x} + z\frac{\partial \varphi_z}{\partial x}\right)\right) z (R+z) dz + \int \ddot{w} z \rho (R+z) dz + \int z^2 \rho \ddot{\varphi}_z (R+z) dz +$$

$$2\pi R w k_1 \frac{h}{2} + 2\pi R k_1 \varphi_z \left(\frac{h}{2}\right)^2 - 2\pi R k_2 \frac{\partial^2 w}{\partial x^2} \frac{h}{2} - 2\pi R k_2 \frac{\partial^2 \varphi_z}{\partial x^2} \left(\frac{h}{2}\right)^2 + 2\pi w k_1 \left(\frac{h}{2}\right)^2 +$$

$$2\pi k_1 \varphi_z \left(\frac{h}{2}\right)^3 - 2\pi k_2 \frac{\partial^2 w}{\partial x^2} \left(\frac{h}{2}\right)^2 - 2\pi k_2 \frac{\partial^2 \varphi_z}{\partial x^2} \left(\frac{h}{2}\right)^3 = 0$$

$$\rightarrow \int \left(Q_{12} z \frac{\partial u}{\partial x} + Q_{12} z^2 \frac{\partial \varphi_x}{\partial x} - Q_{12} z \alpha_{11} T + \frac{Q_{22} z}{R+z} w + \frac{Q_{22} z^2}{R+z} \varphi_z - Q_{22} z \alpha_{22} T + Q_{23} z \varphi_z - Q_{23} z \alpha_{33} T\right) dz +$$

$$\int \begin{bmatrix} Q_{13}R\dfrac{\partial u}{\partial x}+Q_{13}zR\dfrac{\partial \varphi_x}{\partial x}-Q_{13}\alpha_{11}TR+ \\ \dfrac{Q_{23}}{R+z}wR+\dfrac{Q_{23}z}{R+z}\varphi_z R-Q_{23}\alpha_{22}TR+ \\ Q_{33}\varphi_z R-Q_{33}\alpha_{33}TR+Q_{13}z\dfrac{\partial u}{\partial x}+ \\ Q_{13}z^2\dfrac{\partial \varphi_x}{\partial x}-Q_{13}z\alpha_{11}T+\dfrac{Q_{23}z}{R+z}w+ \\ \dfrac{Q_{23}z^2}{R+z}\varphi_z-Q_{23}z\alpha_{22}T+Q_{33}z\varphi_z-Q_{33}z\alpha_{33}T \end{bmatrix} dz$$

$$-\int \begin{bmatrix} Q_{55}Rz\dfrac{\partial \varphi_x}{\partial x}+Q_{55}Rz\dfrac{\partial^2 w}{\partial x^2}+ \\ Q_{55}Rz^2\dfrac{\partial^2 \varphi_z}{\partial x^2}+Q_{55}z^2\dfrac{\partial \varphi_x}{\partial x}+ \\ Q_{55}z^2\dfrac{\partial^2 w}{\partial x^2}+Q_{55}z^3\dfrac{\partial^2 \varphi_z}{\partial x^2} \end{bmatrix} dz +$$

$$\int (R\ddot{w}z\rho+\ddot{w}z^2\rho)dz+\int (Rz^2\rho\ddot{\varphi}_z+z^3\rho\ddot{\varphi}_z)dz+2\pi Rwk_1\frac{h}{2}+2\pi Rk_1\varphi_z\left(\frac{h}{2}\right)^2-$$

$$2\pi Rk_2\frac{\partial^2 w}{\partial x^2}\frac{h}{2}-2\pi Rk_2\frac{\partial^2 \varphi_z}{\partial x^2}\left(\frac{h}{2}\right)^2+2\pi wk_1\left(\frac{h}{2}\right)^2+2\pi k_1\varphi_z\left(\frac{h}{2}\right)^3-2\pi k_2\frac{\partial^2 w}{\partial x^2}\left(\frac{h}{2}\right)^2-$$

$$2\pi k_2\frac{\partial^2 \varphi_z}{\partial x^2}\left(\frac{h}{2}\right)^3=0$$

$$\rightarrow \frac{\partial u}{\partial x}\int Q_{12}zdz+\frac{\partial \varphi_x}{\partial x}\int Q_{12}z^2dz-\alpha_{11}T\int Q_{12}zdz+w\int \frac{Q_{22}z}{R+z}dz+\varphi_z\int \frac{Q_{22}z^2}{R+z}dz$$

$$-$$

$$\alpha_{22}T\int Q_{22}zdz+\varphi_z\int Q_{23}zdz-\alpha_{33}T\int Q_{23}zdz+R\frac{\partial u}{\partial x}\int Q_{13}dz+R\frac{\partial \varphi_x}{\partial x}\int Q_{13}zdz$$

$$-$$

$$\alpha_{11}TR\int Q_{13}dz+wR\int \frac{Q_{23}}{R+z}dz+\varphi_z R\int \frac{Q_{23}z}{R+z}dz-\alpha_{22}TR\int Q_{23}dz+\varphi_z R\int Q_{33}dz$$

$$-$$

$$\alpha_{33}TR\int Q_{33}dz+\frac{\partial u}{\partial x}\int Q_{13}zdz+\frac{\partial \varphi_x}{\partial x}\int Q_{13}z^2dz-\alpha_{11}T\int Q_{13}zdz+w\int \frac{Q_{23}z}{R+z}dz+$$

$$\varphi_z\int \frac{Q_{23}z^2}{R+z}dz-\alpha_{22}T\int Q_{23}zdz+\varphi_z\int Q_{33}zdz-\alpha_{33}T\int Q_{33}zdz-R\frac{\partial \varphi_x}{\partial x}\int Q_{55}zdz$$

$$-$$

$$R\frac{\partial^2 w}{\partial x^2}\int Q_{55}zdz-R\frac{\partial^2 \varphi_z}{\partial x^2}\int Q_{55}z^2dz-\frac{\partial \varphi_x}{\partial x}\int Q_{55}z^2dz-\frac{\partial^2 w}{\partial x^2}\int Q_{55}z^2dz$$

$$-\frac{\partial^2 \varphi_z}{\partial x^2}\int Q_{55}z^3dz+$$

$$R\ddot{w}\int z\rho dz+\ddot{w}\int_{-} z^2\rho dz+R\ddot{\varphi}_z\int z^2\rho dz+\ddot{\varphi}_z\int z^3\rho dz+2\pi Rwk_1\frac{h}{2}+2\pi Rk_1\varphi_z\left(\frac{h}{2}\right)^2$$

$$2\pi Rk_2\frac{\partial^2 w}{\partial x^2}\frac{h}{2}-2\pi Rk_2\frac{\partial^2\varphi_z}{\partial x^2}\left(\frac{h}{2}\right)^2+2\pi wk_1\left(\frac{h}{2}\right)^2+2\pi k_1\varphi_z\left(\frac{h}{2}\right)^3-2\pi k_2\frac{\partial^2 w}{\partial x^2}\left(\frac{h}{2}\right)^2-$$

$$2\pi k_2\frac{\partial^2\varphi_z}{\partial x^2}\left(\frac{h}{2}\right)^3=0$$

$$\rightarrow\delta\varphi_z:\ \frac{\partial u}{\partial x}\int Q_{12}dz+\frac{\partial\varphi_x}{\partial x}\int Q_{12}zdz-\alpha_{11}T\int Q_{12}dz+w\int\frac{Q_{22}}{R+z}dz$$

$$+\varphi_z\int\frac{Q_{22}z}{R+z}dz-$$

$$\alpha_{22}T\int Q_{22}dz+\varphi_z\int Q_{23}dz-\alpha_{33}T\int Q_{23}dz-R\frac{\partial\varphi_x}{\partial x}\int Q_{55}dz-R\frac{\partial^2 w}{\partial x^2}\int Q_{55}dz-$$

$$R\frac{\partial^2\varphi_z}{\partial x^2}\int Q_{55}zdz-\frac{\partial\varphi_x}{\partial x}\int Q_{55}zdz-\frac{\partial^2 w}{\partial x^2}\int Q_{55}zdz-\frac{\partial^2\varphi_z}{\partial x^2}\int Q_{55}z^2dz+R\ddot{w}\int\rho dz$$

$$+$$

$$\ddot{w}\int z\rho dz+R\ddot{\varphi}_z\int z\rho dz+\ddot{\varphi}_z\int z^2\rho dz+2\pi wk_1R+2\pi\frac{h}{2}Rk_1\varphi_z-2\pi Rk_2\frac{\partial^2 w}{\partial x^2}-$$

$$2\pi Rk_2\frac{h}{2}\frac{\partial^2\varphi_z}{\partial x^2}+2\pi wk_1\frac{h}{2}+2\pi\left(\frac{h}{2}\right)^2k_1\varphi_z-2\pi k_2\frac{h}{2}\frac{\partial^2 w}{\partial x^2}-2\pi k_2\left(\frac{h}{2}\right)^2\frac{\partial^2\varphi_z}{\partial x^2}=0$$